Journal of the European Ceramic Society **17** (1997) 879–884

PII: S0955-2219(96)00124-0
0955-2219/97/$17.00

High-Toughness B_4C–AlB_{12} Composites Prepared by Al Infiltration

Wei-Fang Du* & Tadahiko Watanabe

Kyushu National Industrial Research Institute, 807-1 Shuku, Tosu, Saga 841, Japan

(Received 9 May 1996; revised version received 7 June 1996; accepted 15 July 1996)

Abstract

An infiltration technique for fabricating B_4C-matrix composites has been investigated. B_4C–Al composites prepared by infiltration are well densified and have shrinkage of about 0·15%, but the fracture toughness is low. The addition of AlB_{12} has a strong effect in increasing the toughness of B_4C-matrix composites. The high fracture toughness of B_4C–AlB_{12}–Al composites is caused by residual Al and by the behaviour of metastable stress-induced phase transition of AlB_{12} from β-phase to α-phase. The highest hardness (1870 kg/mm^2) and flexural strength (457 MPa) are obtained in B_4C-matrix sample with 8% AlB_{12}. © *1997 Elsevier Science Limited.*

1 Introduction

With good properties, such as high hardness, high melting point, good thermal conductivity and good electrical conductivity, boron carbide ceramics are excellent candidates for neutron absorption materials, wear resistance materials, electrode materials and cutting tools.[1] However, the extreme sensitivity to brittle fracture (K_{IC}=3·2–3·7 MPa m$^{1/2}$) and the high sintering temperature, above 2000°C, are still serious limitations.[2] Full density is usually achieved through costly hot-pressing techniques. Much effort has been expended to overcome this limitation of boron carbide ceramics.[3–5] Recent progress in our laboratory has shown that the mechanical property limitations associated with boride ceramics and the processing problems can be significantly reduced by introducing an AlB_{12} phase and by using an Al infiltration method. In addition, the infiltration processing takes advantage of the low shrinkage and high accuracy to allow complicated shapes in sintered parts.[6,7] The present study was devoted to the preparation of B_4C-matrix composites by introducing an AlB_{12} phase and by using an Al infiltration technique, with the objective of increasing the toughness and decreasing the processing temperatures.

*To whom correspondence should be addressed at: Saitama Laboratory, Research Development Corporation of Japan (JRDC), Shibasita 1-1-56, Kawaguchi-shi, Saitama 333, Japan.

2 Experimental Procedure

Starting materials for the infiltration experiment were high-purity B_4C powder (<300 mesh), and α-phase AlB_{12} powder supplied by Herman C. Stark, Goslar, Germany. First, the B_4C was mixed with AlB_{12} powder in different ratios by weight in a sintered Al_2O_3 mill for 20 min. Then the mixed powder was passed through a sieve. Powder compacts were formed by uniaxially pressing at 18 MPa and then by cold-isostatic pressing (CIP) in a metal mould at 300 MPa at room temperature. An aluminium bath for infiltration was prepared by placing about 10 g Al powder (99·9% purity) in a carbon crucible. The green compacts were put in the carbon bath and infiltrated at various temperatures in vacuum. Figure 1 illustrates schematically our experimental set-up for the infiltration bath. A small amount of about 1–3% CaF_2 additive was dispersed in the Al powder of the infiltration bath to prevent agglomeration of Al after cooling.

After infiltration, the bulk density was measured by the Archimedes' method and the open porosity determinations were performed by impregnation using standard hydrostatic methods. The phases of the composites were examined by X-ray diffraction with a Philips diffractometer using Cu K_α radiation and a scan rate of 1 deg/min. The general morphology of the samples was studied with optical microscopy. The detailed structure of the interfaces was investigated by scanning electron microscope (SEM). In addition, qualitative and quantitative electron probe microanalysis (EPMA) was used for composition determination of phases and analysis of the particle–matrix interface.

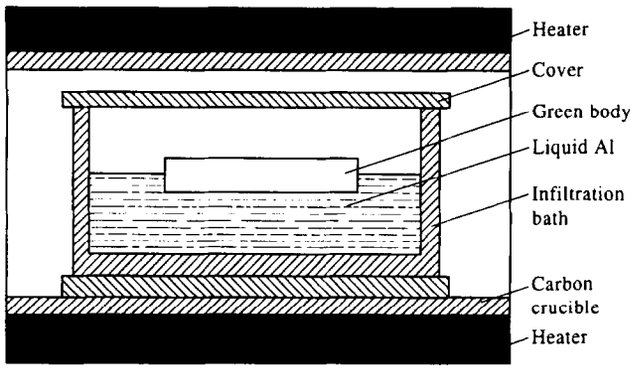

Fig. 1. Experimental set-up for the infiltration bath.

Flexural strength was determined on 2 mm × 4 mm × 14·5 mm samples in three-point flexure using WC-Co support and load rods with an outer span of 10 mm; load speed was 8·3 μm/s. All strength measurements were conducted at room temperature. The Vickers hardness was measured with a load of 100 N on surfaces polished successively with 9, 6, 3 and finally finished using 1 μm diamond paste. The fracture toughness was calculated using the Evans and Charles equation.[8]

3 Results and Discussion

3.1 Factors affecting the infiltration

Infiltration occurred in the samples infiltrated at 1400°C for 1 h. The changes in density and porosity of composites held at various temperatures for 1 h are depicted in Fig. 2. Below 1400°C, the composites exhibited low density with a large amount of porosity, little different from that of the green compact. However, after 1 h at 1400°C in the aluminium bath, the density of the composites increased steeply, yielding a low porosity of 2·1% due to the infiltration of the sample. Figure 3 shows the amounts of infiltrated aluminium phase in samples held at various infiltration temperatures for 1 h, which also clearly confirmed the

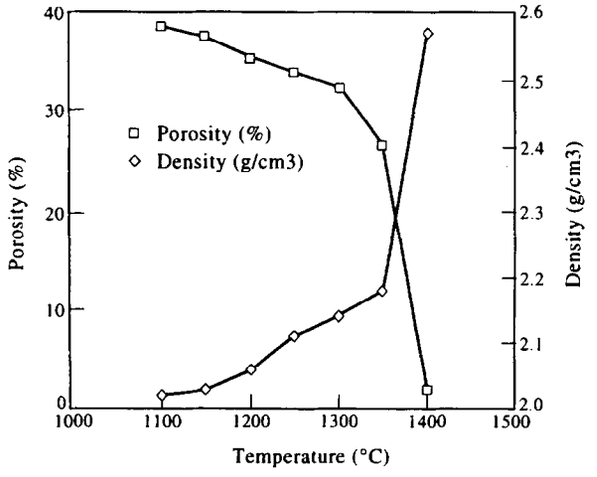

Fig. 2. Density and porosity of the B_4C-matrix composite as a function of temperature.

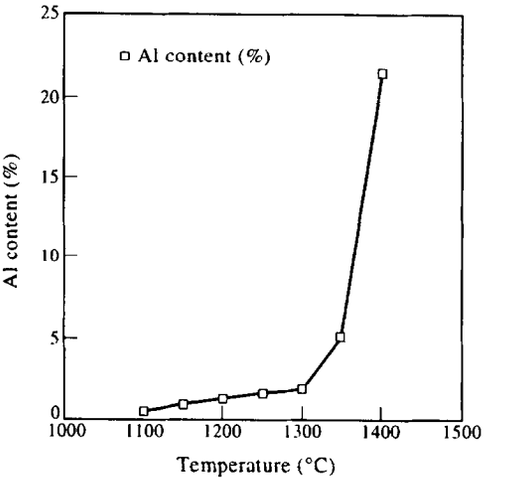

Fig. 3. Amount of infiltrated aluminium phase in samples held at various infiltration temperatures for 1 h.

infiltration occurring at 1400°C after 1 h as the samples contained 21·6 wt% aluminium.

The microstructure of the B_4C–AlB_{12} specimen infiltrated at 1400°C for 1 h, as an example, is shown in Fig. 4(a). It can be seen that B_4C–AlB_{12} is fully infiltrated by aluminium and that there are few pores retained in the specimen. Electron microprobe (EPMA) micrographs show that bonding exists between ceramic particles and aluminium. Figure 4(b)

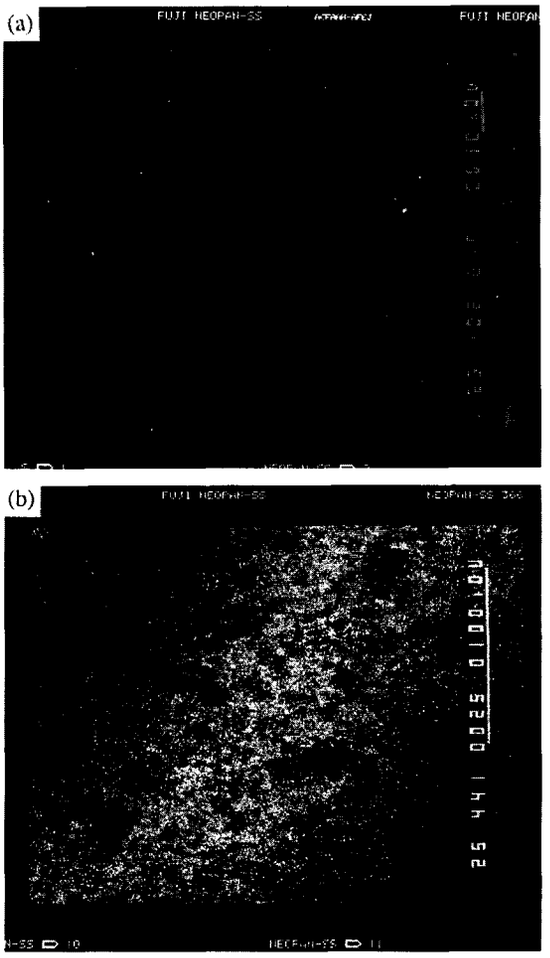

Fig. 4. (a) SEM photograph, and (b) X-ray images of aluminium-rich phase for the B_4C–AlB_{12} composite after infiltration at 1400°C.

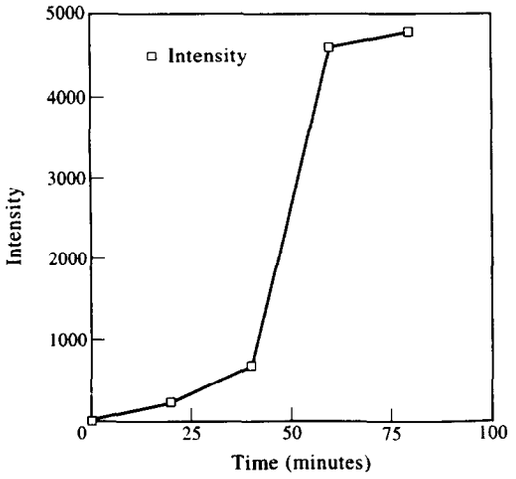

Fig. 5. X-ray intensity of Al phase in B_4C–AlB_{12} composite as a function of infiltration time at 1400°C.

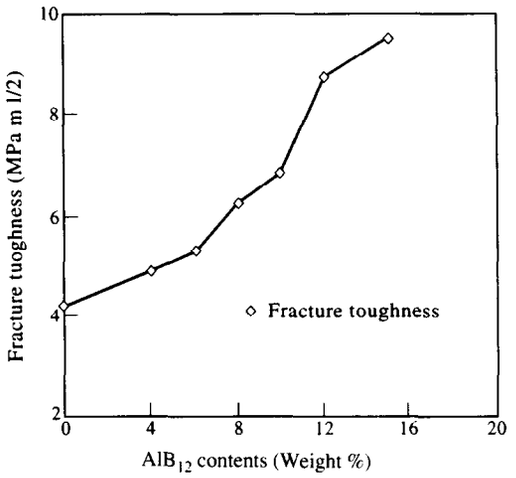

Fig. 7. Effect of AlB_{12} content on the fracture toughness of B_4C–AlB_{12} composites.

corresponds to the X-ray mapping of the Al-rich phases (Al and AlB_{12}) for the specimen infiltrated at 1400°C for 1 h. The densely bright regions correspond to the aluminium-rich phase, which shows a strong coherent bond between the ceramic particles.

The addition of the CaF_2 dispersed in the Al powder bath had a strong effect on the temperature of infiltration. Pure Al powder can infiltrate the B_4C–AlB_{12} green body at the lower temperature of 1150°C. However, a serious problem is that the sample infiltrated in pure Al powder is difficult to remove from the infiltration bath due to the adhesion between the infiltrated sample and the remaining Al after cooling. CaF_2 eliminates this problem and the agglomeration of Al after cooling; however, it also increases the temperature of infiltration to 1400°C due to the decrease in wetting.

The infiltration process also depends on the heating time. The changes in the X-ray intensity of the infiltration phase of aluminium as a function of heating time at 1400°C are shown in Fig. 5. Al begins to infiltrate into the B_4C body when the heating time is above 20 min, and its intensity increases slowly with increasing heating time to 40 min, before increasing rapidly from 40 min to 60 min. After 60 min, the intensity of Al shows little further change with time.

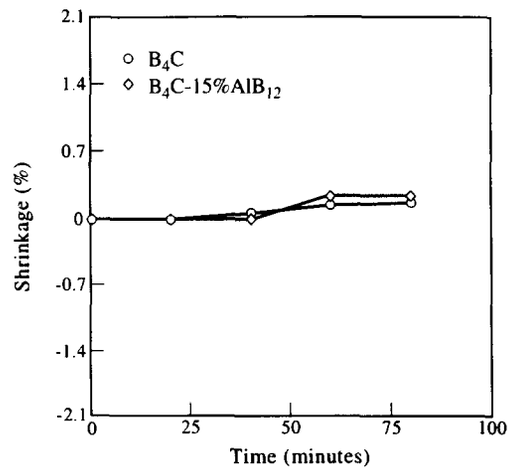

Fig. 6. Shrinkage of B_4C-matrix composites versus infiltration time at 1400°C.

3.2 The characteristics of low shrinkage

Ceramic sintering generally implies large shrinkage, which means it is difficult to achieve high accuracy in the shape and size of sintered parts. Machining operations on sintered parts are expensive and difficult to perform when the parts have a complicated shape. However, the infiltration process used in this study overcomes this limitation. Figure 6 plots the shrinkage versus heating time at 1400°C for B_4C and for a B_4C-AlB_{12} composite respectively. The infiltration process allows a noticeable decrease in shrinkage, which does not exceed 0·15% for the composite infiltrated at 1400°C for 60 min.

3.3 Effect of AlB_{12} and Al contents on the fracture toughness of composites

Figure 7 shows the variation of fracture toughness with the AlB_{12} content of the composites. The B_4C sample prepared by Al infiltration without AlB_{12} addition has low fracture toughness. It is interesting to note that the fracture toughness of the composites increases rapidly as the content of AlB_{12} increases. As shown in Fig. 7, the values of the fracture toughness increase from 4·21 MPa $m^{1/2}$ for the sample without AlB_{12} to 9·54 MPa $m^{1/2}$ for the sample with 15% AlB_{12}.

The relationship between the fracture toughness of the composites and phase transformation of AlB_{12} is still under study. AlB_{12} has two allotropes, a low-temperature tetragonal phase (α-phase) and a high-temperature orthorhombic phase (β-phase), with a transition temperature of 1550°C associated with a 1·7% volume change (the specific gravities of the α-phase and β-phase are 2·557 and 2·60 respectively).[9,10] The starting powder of AlB_{12} is

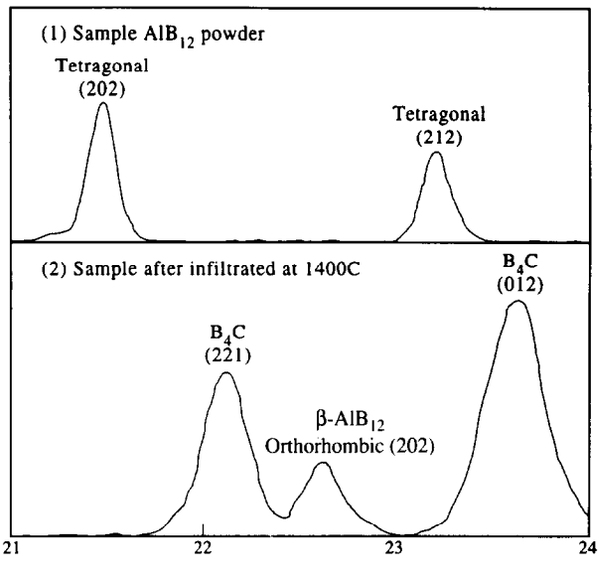

Fig. 8. X-ray pattern, showing the phase transition of AlB_{12} from α-phase to β-phase in the B_4C–AlB_{12} composite after infiltration at 1400°C.

α-phase and the infiltration temperature is lower than that of the phase transition of AlB_{12}; however, the X-ray patterns show that the α-phase changes into the β-phase in composites infiltrated at 1400°C for 1 h, as shown in Fig. 8.

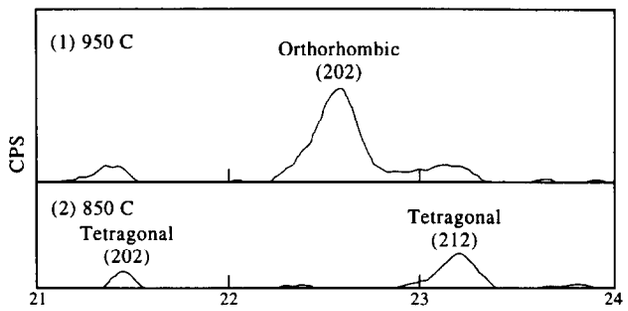

Fig. 9. X-ray pattern showing the phase transition from α-phase to β-phase for AlB_{12} particles dispersed in 60% Al sintered at 950°C.

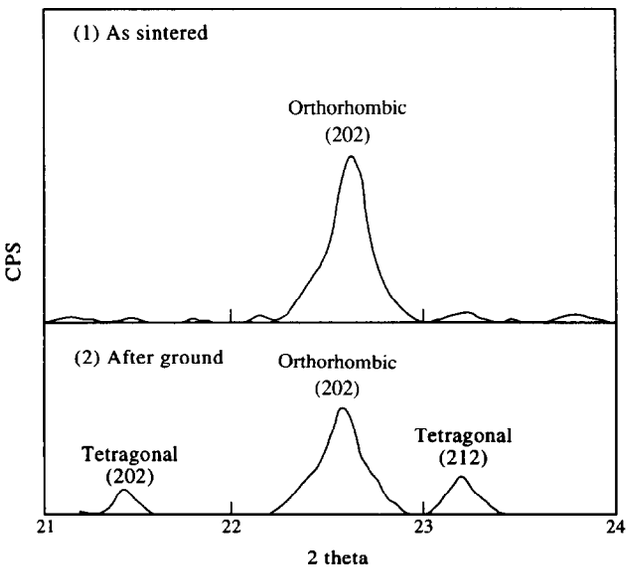

Fig. 10. Influence of stress on the transition from metastable β-phase to α-phase for AlB_{12} particles dispersed in 60% Al-matrix sintered at 950°C.

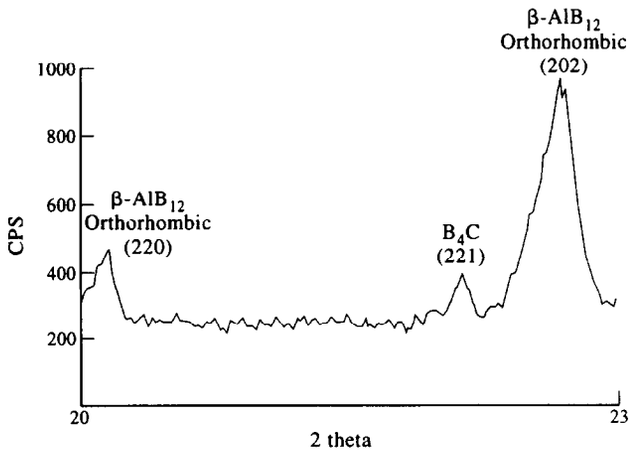

Fig. 11. X-ray pattern showing metastable β-phase AlB_{12} stabilized temporarily by boron carbide in AlB_{12}–20%B_4C sample infiltrated at 1200°C.

Furthermore, we found that phase transition from α to β for AlB_{12} could take place at a temperature as low as 950°C when the α-phase AlB_{12} particles were dispersed in an aluminium matrix (Fig. 9). However, this β-phase AlB_{12}, which is under compressive stress due to the thermal shrinkage of Al-matrix on cooling, is metastable at room temperature and can be transformed readily to the α-phase after the release of the compressive stress on the particles of β-phase. An as-sintered surface of AlB_{12} with 60% volume Al is free of the α-phase, but the β-phase occurs after grinding, as shown in Fig. 10. This process induces a transverse rupture stress at the surface,[11] which removes the compressive stress on the particles of the β-phase to some extent, allowing transition to the α-phase. In addition, we also observed metastable β-phase AlB_{12} stabilized by boron carbide at as low a temperature as 1200°C (Fig.11).

The behaviour of this metastable stress-induced phase transition between the α-phase and β-phase of AlB_{12} where the high-temperature phase can be temporarily stabilized by the additive B_4C is just like that of the t- to m-phase transition in zirconia,[12–15] which exhibits martensitic behaviour and thus is thought to contribute greatly to high fracture toughness, because the very high rate of the martensitic phase transition under applied

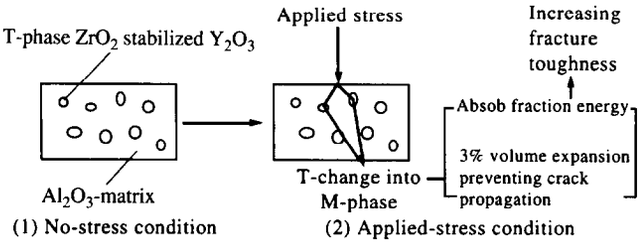

Fig. 12. A schematic drawing showing the toughening mechanism of ZrO_2 in Al_2O_3–$ZrO_2(Y_2O_3)$ composites.

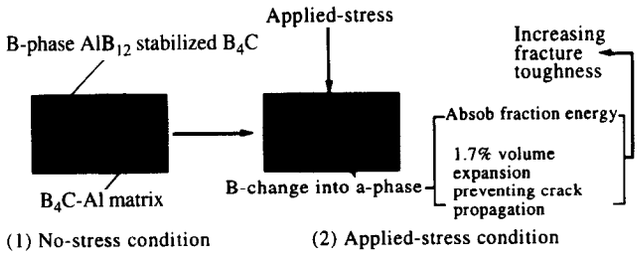

Fig. 13. A schematic drawing showing the toughening mechanism of AlB_{12} for B_4C–AlB_{12} composites.

stress, which is about two to three times faster than the rate of crack extension, can quickly absorb fracture energy. In addition, the volume expansion of about 1·7% during the stress-induced phase transition enhances the resistance to crack propagation, as shown schematically in Figs 12 and 13.

The high fracture toughness of the B_4C–15% AlB_{12} composite can also come from the greater content of residual Al after infiltration. Figure 14 shows the amount of residual Al in the samples with different amounts of AlB_{12}. This increases from 21·6% for the B_4C sample to 27·5% for the B_4C–15% AlB_{12} sample.

3.4 Effect of AlB_{12} content on the bending strength and hardness of the composites

The bending strength and the hardness of the B_4C–AlB_{12} composites as a function of AlB_{12} content is plotted in Fig. 13. The B_4C sample without AlB_{12} additive has a bending strength of about 278 MPa and a hardness of about 1127 kg/mm^2, respectively. With increasing content of AlB_{12}, the bending strength and the hardness of the composites increase rapidly and reach a maximum of 457 MPa and 1870 kg/mm^2 for the sample with 8% AlB_{12} additive. Presumably, the increase in strength and hardness

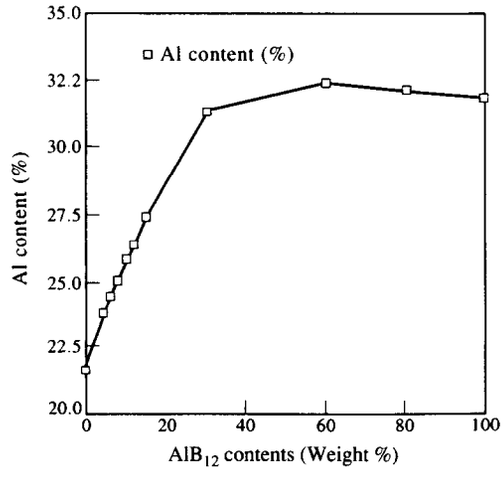

Fig. 14. Variation of amount of residual Al in the samples with different amounts of AlB_{12}.

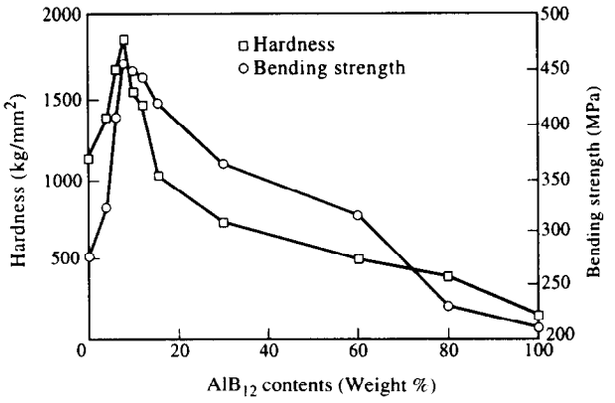

Fig. 15. Bending strength and hardness of the B_4C–AlB_{12} composites as a function of AlB_{12} content.

of the sample with increasing AlB_{12} is due to the lower porosity as shown in Fig. 15. Above 8% AlB_{12}, the bending strength and hardness of composites decline with increasing AlB_{12} content.

4 Conclusions

(1) B_4C-matrix composites have been fabricated by infiltration technique in vacuum. The samples are well densified after infiltration in an aluminium bath at 1400°C for 1 h.

(2) B_4C-matrix composites prepared by the infiltration method provide a dramatic decrease in shrinkage during sintering. The lowest shrinkage is about 0·15%.

(3) There exists a metastable stress-induced phase transition between the α-phase and β-phase of AlB_{12} below 1550°C which has not been earlier reported. In addition, the metastable β-phase AlB_{12} can be stabilized temporarily by the addition of boron carbide below 1550°C.

(4) The fracture toughness of the B_4C–AlB_{12} composites increases rapidly with increasing

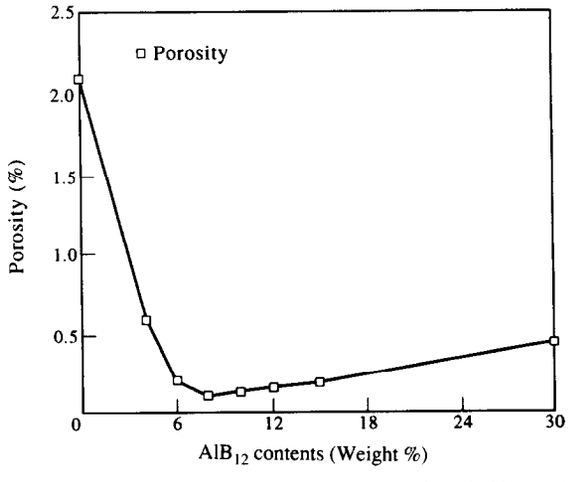

Fig. 16. Porosity of the B_4C–AlB_{12} composites infiltrated at 1400°C for 1 h as a function of AlB_{12} content.

content of AlB_{12}. This effect is perhaps related to the behaviour of the metastable stress-induced phase transition between the α-phase and β-phase of AlB_{12}. A maximum toughness value of about 9·54 MPa $m^{1/2}$ is achieved for the sample with 15% AlB_{12}.

(5) The AlB_{12} additive also strongly affects the bending strength and the hardness of B_4C–AlB_{12} composites. The AlB_{12} content providing the maximum bending strength and hardness in B_4C-AlB_{12} composites is about 8%.

Acknowledgements

This study was supported by the Guest Researcher Program of the Agency of Industrial Science and Technology of Japan and the STA fellowship program of Japan. The authors wish to express appreciation to Dr C. N. Xu, Dr M. Komatsu, Dr M. Akiyama, Dr W. P. Tai and Dr K. Shobu for their help and suggestions.

References

1. Beauvy, M. and Angers, R., Mechanisms of hot-pressing of boron carbide powders. In *Science of Ceramics*, Vol. 10, ed. H. Hausner. Deutsche Keramische Gessellschaft, Weiden, FRG, 1980, pp. 279–286.
2. de With, G., High-temperature fracture of boron carbide: Experiments and simple theoretical models. *J. Mater. Sci.*, 1984, **19**, 457–466.
3. Halverson, D. C., Pyzik, A. J. and Aksay, I. A., Processing and microstructural characterization B_4C/Al Cermets. *Ceram. Eng. Sci. Proc.*, 1985, **6**, 7–8.
4. Halverson, D. C., Pyzik, A. J., Aksay, I. A. and Snowden, W. E., Processing of boron carbide–aluminium composites. *J. Am. Ceram. Soc.*, 1989, **72**, 775–780
5. Pyzik, A. J. and Beaman, D. R., Al–B–C phase development and effects on mechanical properties of B_4C/Al-derived composites. *J. Am. Ceram. Soc.*, 1995, **78**, 305–312.
6. Yang, X. F. and Xi, X. M., SiC–Al–Si composites by rapid pressureless infiltration in air. *J. Mater. Res.*, 1995, **10**, 2415–2417.
7. Lequeux, N., Larose, P. and Boch, P., Low-shrinkage refractories by an infiltration technique. *J. Euro. Ceram. Soc.*, 1994, **14**, 23–27.
8. Evans, A. G. and Charles, E. A., Fracture toughness determinations by indention. *J. Am. Ceram. Soc.*, 1976, **59**, 371–372.
9. Carison, O. N., The Al–B (aluminium–boron) system. *Bulletin of Alloy Phase Diagrams*, 1990, **11**, 560–567.
10. Matkovich, V. I., Economy, J. and Giese, R. F., Presence of carbon in aluminium borides. *J. Am. Chem. Soc.*, 1964, **86**, 2337–2340.
11. Garvie, R. C., Hannink, R. H. and Pascoe, R. T., Ceramic steel. *Nature*, 1972, **258**, 703–704.
12. McMeeking, R. M. and Evans, A. G., *J. Am. Ceram. Soc.*, 1982, **65**, 242.
13. Watanabe, T. and Shobu, K., *J. Am. Ceram. Soc.*, 1985, **83**, C34.
14. Shobu, K., Watanabe, T., Drennan, J., Hannink, R. H. and Swain, M. V., *Advance in Ceramics*, Vol. 24, *Science and Technology of Zirconia III*, 1988, p. 1091.
15. Watanabe, T., Shobu, K. and Tani, E., Effect of ZrO_2 addition on the mechanical properties of TiB ceramics. *J. Japan Soc. Powder and Powder Metallurgy*, 1994, **41**, 43–47.